Formation of the three-dimensional geometry of the red blood cell membrane

P. G. Hasitha Nayanajith[1] Suvash C. Saha[2]
YuanTong Gu[3]

(Received 18 December 2013; revised 18 March 2014)

Abstract

Red blood cells (RBCs) are nonnucleated liquid capsules, enclosed in deformable viscoelastic membranes with complex three dimensional geometrical structures. Generally, RBC membranes are highly incompressible and resistant to areal changes. However, RBC membranes show a planar shear deformation and out of plane bending deformation. The behaviour of RBCs in blood vessels is investigated using numerical models. All the characteristics of RBC membranes should be addressed to develop a more accurate and stable model. This article presents an effective methodology to model the three dimensional geometry of the RBC membrane with the aid of commercial software COMSOL Multiphysics 4.2a and Fortran programming. Initially, a mesh is generated

http://journal.austms.org.au/ojs/index.php/ANZIAMJ/article/view/7820 gives this article, Published May 7, 2014, as part of the Proceedings of the 11th Biennial Engineering Mathematics and Applications Conference. ISSN 1446-8735.

for a sphere using the COMSOL Multiphysics software to represent the RBC membrane. The elastic energy of the membrane is considered to determine a stable membrane shape. Then, the actual biconcave shape of the membrane is obtained based on the principle of virtual work, when the total energy is minimised. The geometry of the RBC membrane could be used with meshfree particle methods to simulate motion and deformation of RBCs in micro-capillaries.

Contents

1 Introduction

Bone marrow produces the red blood cells (RBCs) of the blood. RBCs eject their nuclei in the early stages of maturity [1]. Healthy matured human RBCs have a discoidal biconcave shape (see Figures 7 and 8) and they contain a viscous fluid called cytoplasm. The cytoplasm is rich in haemoglobin, which carries and delivers oxygen to the different tissues of the body. The discoidal biconcave shape of the RBCs provides a high surface to volume ratio. This high surface to volume ratio aids to increase the efficiency of oxygen diffusion through the RBC membrane. The viscoelastic membrane of the RBC consists of a lipid bilayer, and is supported by a mesh-like cytoskeleton. The mesh-like cytoskeleton is formed by a network of spectrin proteins linked by short filaments of actin [2, 3]. Due to this complex three dimensional geometric structure, RBCs exhibit various types of motions and deformed shapes when they flow within the cardiovascular system.

Over the last few decades, a number of numerical models were proposed to explain and predict RBC behaviour in the microvessels [4]. However, most of the models were two dimensional and were unable to capture the three dimensional nature of RBC motion and deformation. In recent years, particle methods were used to model RBC behaviour in microvessels [5, 6, 7], since the motion, deformation and the fluid structure interacion of RBCs are easily modelled. In reality, the motion and deformation of the RBCs are highly three dimensional, as they exhibit three dimensional deformations in microvessels [8]. Therefore, simplified two dimensional models are not enough to capture the actual behaviour of RBCs in microvessels.

This study presents an effective methodology to form the three dimensional geometry of the RBC membrane with the aid of commercial software COMSOL Multiphysics 4.2a and Fortran programming. Initially, a mesh is generated for a sphere using the COMSOL Multiphysics software, as shown in Figure 1, to represent the RBC membrane before ejecting the nucleus. Then, the energy functions related to in-plane deformation, bending and area are applied to the membrane particles with a penalty function to represent the volume constraint. The forces acting on each membrane particle are then calculated based on the principle of virtual work, and they are formulated using a Fortran code. Energy curves show that the RBC membrane energy is minimised when it has the discoidal biconcave shape. This RBC membrane geometry could be used with meshfree particle methods to simulation of the motion and deformation of a RBC in micro-capillaries.

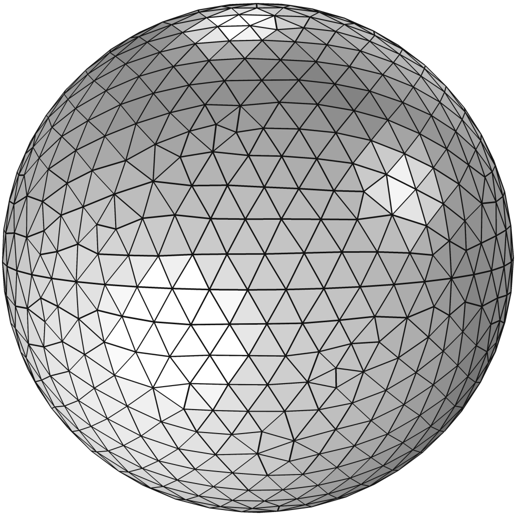

Figure 1: Mesh generated by COMSOL Multiphysics software.

2 Methodology

The RBC membrane is represented by a spring network [9]. Initially, it is assumed that the shape of the RBC membrane is spherical with a radius of 3.27 μm. A spherical geometry is built by COMSOL Multiphysics 4.2a software, using the "surface" option for the object type. Then, a user controlled mesh is generated for the spherical surface with the same minimum and maximum element sizes (0.5 μm), to ensure the size and shape of the triangles remain as similar as possible (see Figure 1). Finally, the mesh is exported as a ".mphtxt" file to obtain the node coordinates and the node numbers. The exported mesh file shows that the spherical surface is divided into 774 mesh points, or nodes, and 1544 elements. The coordinates of the 774 nodes and the node numbers, which generate the 1544 triangular elements, are extracted for further processing with a Fortran code. Particles with finite masses are placed on each node.

2.1 In-plane deformation

The RBC membrane shows in-plane deformation when the membrane is subjected to an external force field. To represent the in-plane deformation (planar shear), elastic springs S are used to interconnect the particle on each node, which generate the triangular elements of the mesh. The length changes in these springs change the stored energy

$$E_S = \frac{1}{2} K_S \sum_{n=1}^{N_S} (L_n - L_{n0})^2 \,, \tag{1}$$

where K_S is the spring constant for stretching/compression and N_S is the number of springs, while L_n and L_{n0} are the deformed length and the reference length of the nth spring, respectively. The reference length is set to the initial length, when the springs are at rest. Assume that the ith particle is connected to six neighbouring particles by six elastic springs as in Figure 2. The forces (ith) acting on the ith particle due to any change in the length of the springs are calculated on the basis of the principle of virtual work:

$$F_{i,S} = -K_S \frac{\partial}{2\partial \mathbf{r}_i} \sum_{n=1}^{6} (L_n - L_{n0})^2 \,, \tag{2}$$

where $\mathbf{r}_i$ is the position vector of the ith particle. The force component in the x direction, acting on the ith particle due to the change in the length of the S_1 spring is $F_{i,S_1,x}$ and it is a function of the coordinates of the ith particle:

$$F_{i,S_1,x} = -K_S (L_{S_1} - L_{S_10}) \frac{x_i - x_1}{L_{S_1}} \,. \tag{3}$$

2.2 Bending deformation

The RBC membrane seeks to minimise the bending energy to obtain a stable shape, so that the membrane is locally flat. The elastic bending energy stored

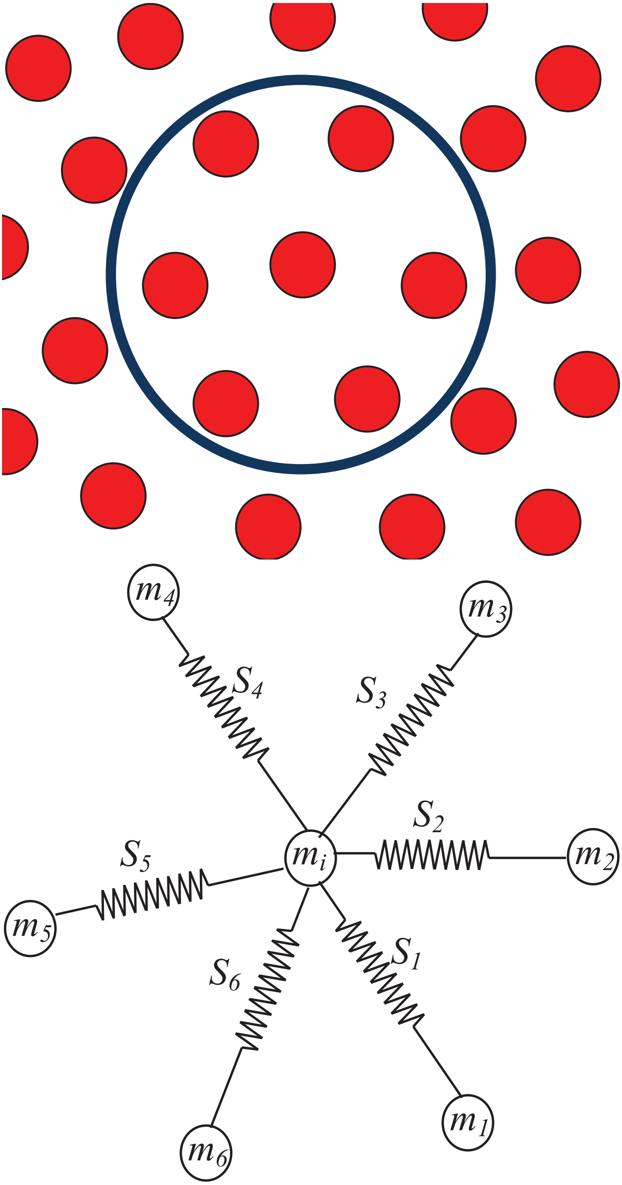

Figure 2: Particle (node) locations on the RBC membrane.

in the RBC membrane due to the bending is

$$E_B = \frac{1}{2} K_B \sum_{n=1}^{N_B} L_n \tan^2(\theta_n - \theta_{n0}) \,, \tag{4}$$

where θ_n is the angle between two normal vectors of neighbouring triangles formed by elastic springs for stretching/compression and θ_{n0} is the reference angle between the above two triangles without deformation (see Figure 3). Also, L_n is the length of the common side of the two triangles and K_B is the spring constant for bending. The number of neighbouring triangles is N_B and is equal to the number of elastic springs used to represent the stretching/compression forces. Here, θ_{n0} is set to zero and equation (4) is rewritten as

$$E_B = \frac{1}{2} K_B \sum_{n=1}^{N_B} L_n \frac{1 - \hat{\mathbf{n}}_{ijk} \cdot \hat{\mathbf{n}}_{ilj}}{1 + \hat{\mathbf{n}}_{ijk} \cdot \hat{\mathbf{n}}_{ilj}} \,, \tag{5}$$

where $\hat{\mathbf{n}}_{ijk}$ and $\hat{\mathbf{n}}_{ilj}$ are the unit normal vectors for two neighbouring triangles $\triangle IJK$ and $\triangle JIL$, respectively, as shown in Figure 3. The force acting on the ith particle due to the bending deformation is

$$\mathbf{F}_{i,B} = -K_B \frac{\partial}{2\partial \mathbf{r}_i} \sum_{n=1}^{NB} L_n \frac{1 - \hat{\mathbf{n}}_{ijk} \cdot \hat{\mathbf{n}}_{ilj}}{1 + \hat{\mathbf{n}}_{ijk} \cdot \hat{\mathbf{n}}_{ilj}} \,. \tag{6}$$

2.3 Area incompressibility

The number of lipids per area of the RBC membrane is constant and the RBC membrane shows a high resistance to changes in surface area. The elastic energy generated by the RBC membrane due to a change in total RBC membrane area from reference area A_0 to A is

$$E_A = \frac{1}{2} K_A A_0 \left(\frac{A - A_0}{A_0} \right)^2 , \tag{7}$$

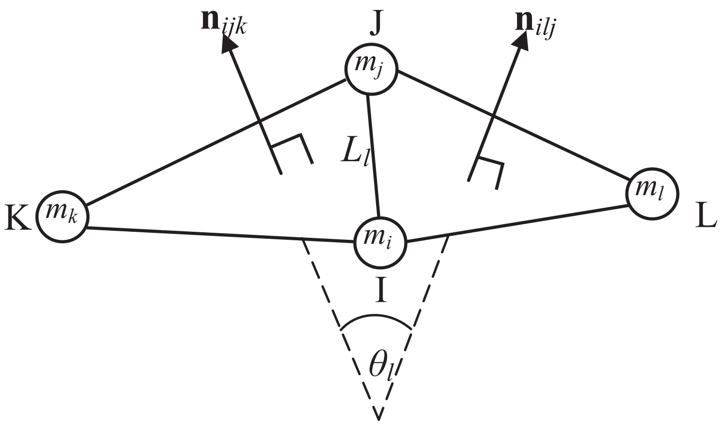

Figure 3: Angle between two neighbouring triangles.

where K_A is the area expansion moduli for the whole membrane.

Further, local area incompressibility should be considered and the energy generation due to the changes in the local area of the triangles A_n, formed by elastic springs for stretching/compression is

$$E_a = \frac{1}{2} K_a A_{n0} \sum_{n=1}^{Na} \left(\frac{A_n - A_{n0}}{A_{n0}} \right)^2 , \tag{8}$$

where A_{n0} is the reference value for the initial local area of the triangle and K_a is the area expansion moduli for the triangular element. The force acting on the ith particle due to the local area incompressibility and the total area incompressibility ($\mathbf{F}_{i,a}$ and $\mathbf{F}_{i,A}$, respectively) are calculated based on the principle of virtual work:

$$\mathbf{F}_i = -\frac{\partial E}{\partial \mathbf{r}_i} . \tag{9}$$

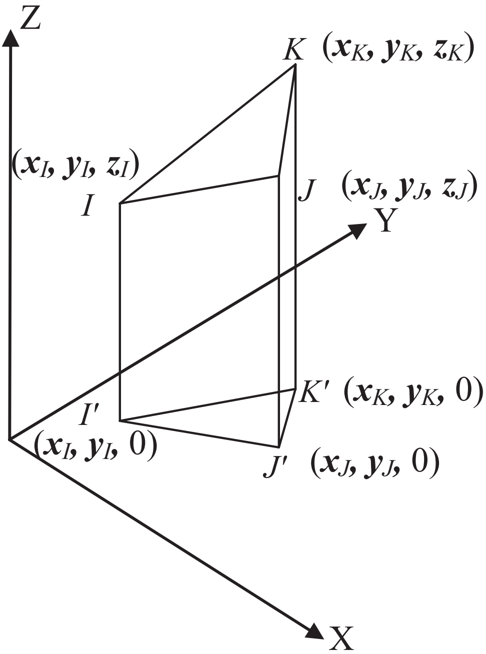

Figure 4: The RBC is divided into triangular prisms to calculate its volume.

2.4 Volume constraint

The total volume V enclosed by the RBC membrane is equal to the volume of a healthy matured RBC. The energy generation, due to the change in the total enclosed volume is

$$E_V = \frac{1}{2} K_V V_0 \left(\frac{V - V_0}{V_0} \right)^2 , \tag{10}$$

where V_0 is the reference volume and K_V is the penalty coefficient [9] to maintain the V as V_0. To calculate the total volume of the RBC, the RBC membrane is divided into triangular oblique prisms as shown in Figure 4. The volumes of the prisms are individually calculated, and then the sum is taken. Assume that the particles $I(x_I, y_I, z_I)$, $J(x_J, y_J, z_J)$ and $K(x_K, y_K, z_K)$ generate the triangle IJK. The projected area vector $\mathbf{A}_p$ of the IJK triangle on the xy plane is equal to the area of the $I'J'K'$ triangle (see Figure 4), and is proportional to the cross product of the two vectors $\mathbf{I'J'}$ and $\mathbf{J'K'}$:

$$\mathbf{A}_p = \left(\frac{\mathbf{I'J'} \times \mathbf{J'K'}}{2} \right). \tag{11}$$

To calculate the projected area, the counter-clockwise orientation of the three triangle points and the real value of the cross product are used. Thus, the error due to the orientation is omitted. Then the volume of the prism is

$$V_p = \left(\frac{\mathbf{I'J'} \times \mathbf{J'K'}}{2} \right) \cdot \left(\frac{z_I + z_J + z_K}{3} \right). \tag{12}$$

The force acting on the ith particle due to the volume constraint ($\mathbf{F}_{i,V}$) is calculated on the basis of principle of virtual work (see equation (9)).

2.5 Equation of motion

The total force acting on the ith particle is the sum of all above mentioned forces:

$$\mathbf{F}_i = \mathbf{F}_{i,S} + \mathbf{F}_{i,B} + \mathbf{F}_{i,A} + \mathbf{F}_{i,a} + \mathbf{F}_{i,V}\,. \tag{13}$$

The mass of each particle is $5\,\mu g$ and the time step is 1×10^{-5} s over a temporal domain of 250 s. A Fortran 90 computer code calculated the forces acting on the RBC membrane particles and Intel Visual Fortran Composer XE compiled the code. Results are analysed using Tecplot 360 software. The velocity and the position of each particle are updated by using the acceleration $\ddot{\mathbf{r}}$, which is related to the total force by

$$\mathbf{F}_i = m\ddot{\mathbf{r}}. \tag{14}$$

Other parameters are given in Table 1.

Table 1: Simulation parameters.

Parameter	$K_S(N/m)$	$K_B(N)$	$K_A(N/m)$	$K_a(N/m)$	$K_V(N/m^2)$
Value	1×10^{-6}	1×10^{-11}	5×10^{-3}	5×10^{-5}	2×10^{0}

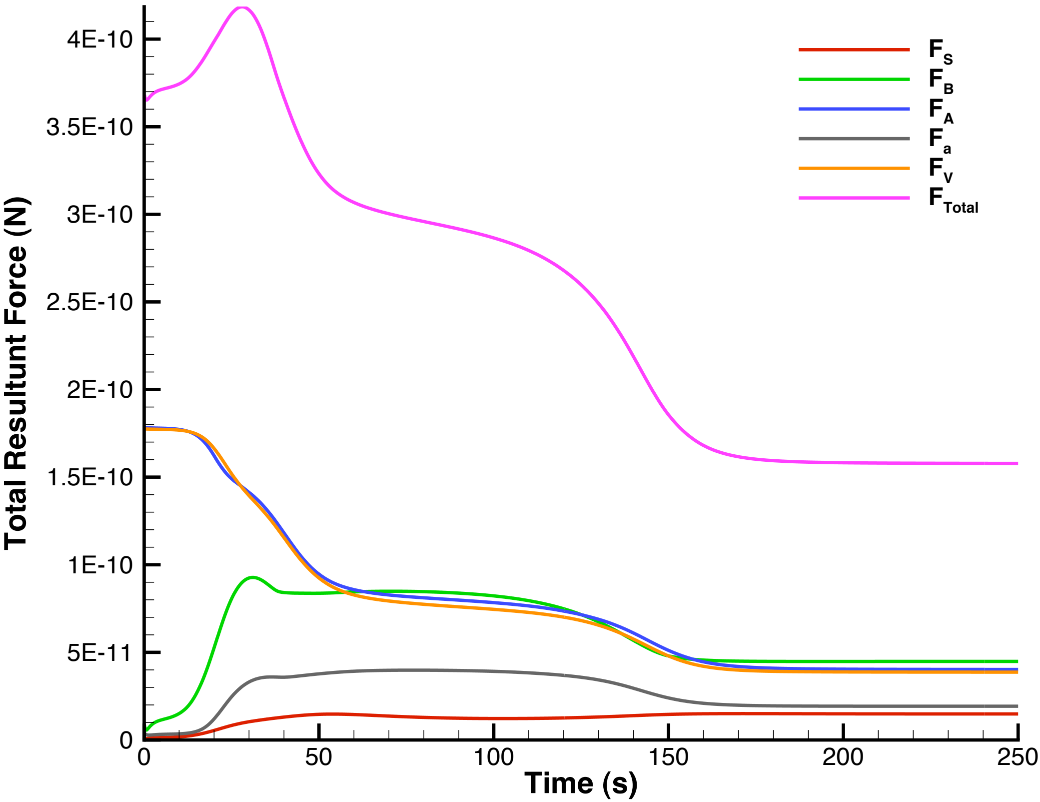

Figure 5: Variation of total forces.

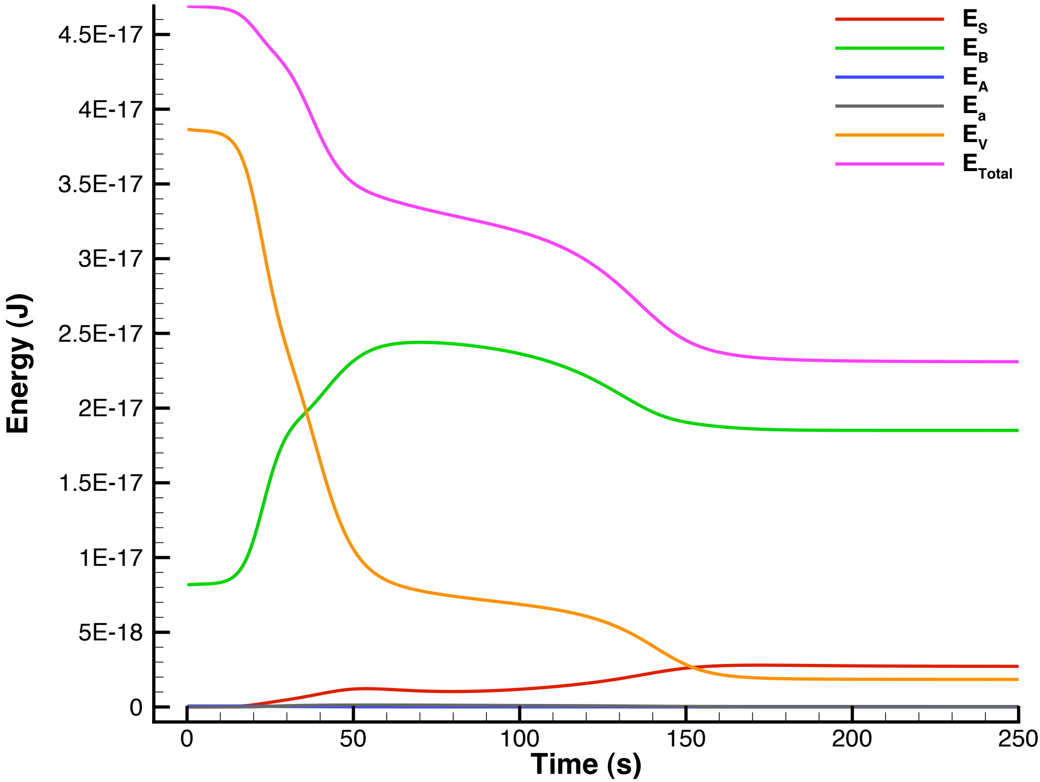

Figure 6: Variation of energy.

Initially, the RBC membrane experiences very high forces, then gradually the total resultant force acting on the membrane decreases (see Figure 5). After 200 s, the forces acting on the membrane become stable and do not show any variation with time. The variation of the energy with time exhibits similar behaviour, as shown in Figure 6. The typical biconcave discoidal shape of a matured healthy RBC is obtained at $t = 200$ s (see Figure 7). Since the energy and forces do not change with time after $t = 200$ s, the RBC membrane does not show any shape change. Therefore, after $t = 200$ s, the RBC membrane has reached a stable shape. This biconcave discoidal shape matches with

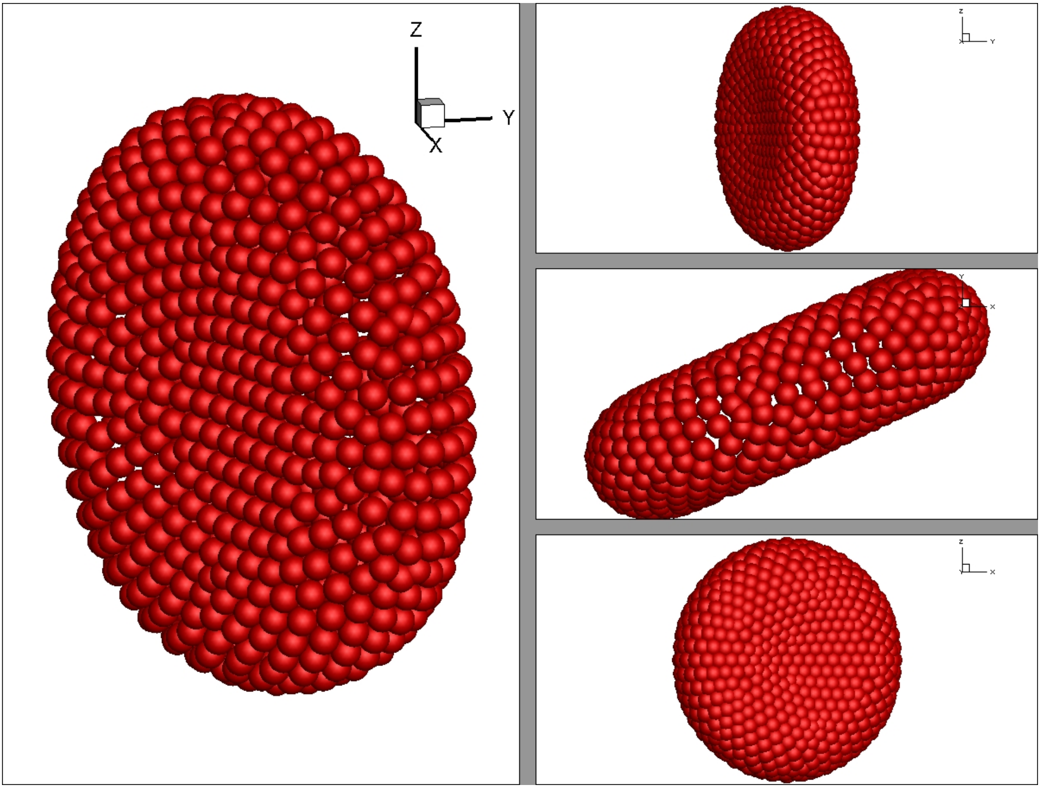

Figure 7: Final shape of the RBC membrane.

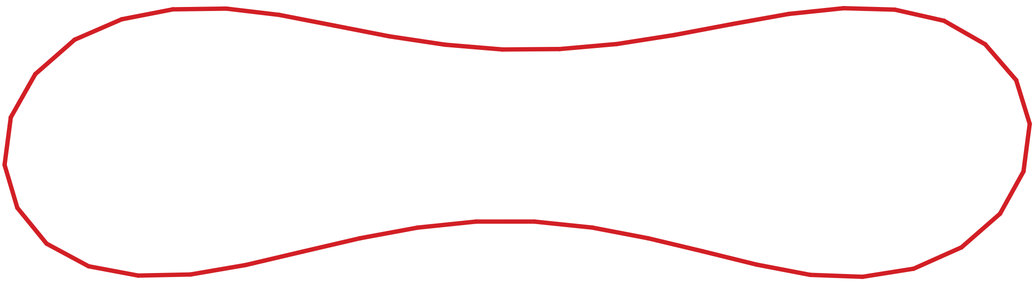

Figure 8: Cross sectional area of the final shape the RBC membrane.

scanning electron microscope images of RBCs [10]. A cross section of the final three dimensional shape of the RBC membrane gives the two dimensional biconcave shape of the RBC and its aspect ratio is close to the aspect ratio [11] of an average healthy RBC (see Figure 8).

3 Conclusions

This is an effective methodology to model the three dimensional geometry of the RBC membrane. The RBC membrane is discretized into a finite number of particles with mass. Then, the energy of the RBC membrane is considered and the stable biconcave discoidal shape of the RBC is obtained, when the total energy of the membrane is minimised. Variation of energy and forces with time confirm that the RBC membrane is stable after 200 s. This stable RBC geometry can be used with particle methods. It is expected that this RBC model can be used with smoothed particle hydrodynamics to simulate the motion and deformation of the RBCs when the blood flows through micro-capillaries.

Acknowledgements Support provided by the ARC Future Fellowship grant (FT100100172) and the High Performance Computer (HPC) resources in Queensland University of Technology (QUT) are gratefully acknowledged.

References

[1] J. B. Freund and H. Zhao. A High-Resolution Fast Boundary-Integral Method for Multiple Interacting Blood Cells. In *Computational Hydrodynamics of Capsules and Biological Cells*, page 71. Chapman and Hall, 2010. C81

[2] C. Pozrikidis. Numerical simulation of the flow-induced deformation of red blood cells. *Ann. Biomed. Eng.*, 31(10):1194–1205, 2003. doi:10.1114/1.1617985 C82

[3] D. A. Fedosov, B. Caswell, and G. E. Karniadakis. A multiscale red blood cell model with accurate mechanics, rheology, and dynamics. *Biophys. J.*, 98(10):2215–2225, 2010. doi:10.1016/j.bpj.2010.02.002 C82

[4] H. N. P. Gallage, Y. T. Gu, S. C. Saha, W. Senadeera, and A. Oloyede. Numerical simulation of red blood cells' motion : a review. In Y. T. Gu and S. C. Saha, editors, *4th International Conference on Computational Methods (ICCM 2012)*, Crowne Plaza, Gold Coast, QLD, November 2012. C82

[5] T. W. Pan and T. Wang. Dynamical simulation of red blood cell rheology in microvessels. *Int. J. Numer. Anal. Mod.*, 6:455–473, 2009. C82

[6] K. I. Tsubota, S. Wada, H. Kamada, Y. Kitagawa, R. Lima, and T. Yamaguchi. A particle method for blood flow simulation: application to flowing red blood cells and platelets. *Journal of the Earth Simulator*, 5:2–7, 2006. http://www.jamstec.go.jp/esc/publication/journal/jes_vol.5/index.html C82

[7] H. N. P. Gallage, Y. T. Gu, S. C. Saha, W. Senadeera, and A. Oloyede. Numerical simulation of red blood cells' deformation using sph method. In Y. T. Gu and S. C. Saha, editors, *4th International Conference on Computational Methods (ICCM 2012)*, Crowne Plaza, Gold Coast, QLD, November 2012. C82

[8] T. W. Secomb, B. Styp-Rekowska, and A. R. Pries. Two-dimensional simulation of red blood cell deformation and lateral migration in microvessels. *Ann. Biomed. Eng.*, 35(5):755–765, 2007. doi:10.1007/s10439-007-9275-0 C82

[9] K. I. Tsubota and S. Wada. Elastic force of red blood cell membrane during tank-treading motion: Consideration of the membrane's natural state. *Int. J. Mech. Sci.*, 52(2):356–364, 2010. doi:10.1016/j.ijmecsci.2009.10.007 C83, C88

[10] M. Bessis. Red Cell Shapes. An Illustrated Classification and its Rationale. In M. Bessis, R. I. Weed, P. F. Leblond, Eds., *Red Cell Shape*, pages 1–25. Springer Berlin Heidelberg, 1973. doi:10.1007/978-3-642-88062-9_1 C93

[11] K. Tsukada, E. Sekizuka, C. Oshio, and H. Minamitani. Direct measurement of erythrocyte deformability in diabetes mellitus with a transparent microchannel capillary model and high-speed video camera system. *Microvasc. Res.*, 61(3):231–239, 2001. doi:10.1006/mvre.2001.2307 C93

Author addresses

1. **P. G. Hasitha Nayanajith**, School of Chemistry, Physics and Mechanical Engineering, Queensland University of Technology, Brisbane, Queensland, Australia 4000, Australia.
2. **Suvash C. Saha**, School of Chemistry, Physics and Mechanical Engineering, Queensland University of Technology, Brisbane, Queensland, Australia 4000, Australia.
3. **YuanTong Gu**, School of Chemistry, Physics and Mechanical Engineering, Queensland University of Technology, Brisbane, Queensland, Australia 4000, Australia
   mailto:yuantong.gu@qut.edu.au